Preparation and Performance Evaluation of Composite Hollow Fiber Membrane for SO_2 Separation

KeeHong Kim
Korea Institute of Energy Research, Yuseong-gu, Daejeon, Republic of Korea

Dept. of Chemical and Biomolecular Engineering, Yonsei University, Seodaemun-gu, Seoul, Republic of Korea

SeongUk Hong
Dept. of Chemical and Biological Engineering, Hanbat National University, Yuseong-gu, Daejeon, Republic of Korea

JongHak Kim
Dept. of Chemical and Biomolecular Engineering, Yonsei University, Seodaemun-gu, Seoul, Republic of Korea

HyungKeun Lee
Korea Institute of Energy Research, Yuseong-gu, Daejeon, Republic of Korea

DOI 10.1002/aic.14424
Published online March 7, 2014 in Wiley Online Library (wileyonlinelibrary.com)

Emission of sulfur dioxide (SO_2) from coal power plants has to be controlled and minimized to reduce environmental risk. This study aimed to investigate the hollow fiber composite membrane was used for the removal of SO_2 from a SO_2/CO_2/N_2 mixed gas. Moreover, for the improvement of SO_2 removal efficiency, the polyetherimide (PEI) membrane was coated with poly(vinyl chloride)-graft-poly(oxyethylene methacrylate) (PVC-g-POEM). The PVC-g-POEM/PEI composite hollow fiber membrane was extensively characterized by various techniques including scanning electron microscopy, Fourier transform infrared spectroscopy, and atomic force microscopy. Experiments with permeation of SO_2, CO_2, N_2, and a ternary gas mixture were carried out to observe membrane behavior in response to different operating conditions. As a result, permeance of SO_2 was 105–2705 GPU and selectivity of SO_2/CO_2 was 3.9–175.6. From the mixed gas separation experiment, the maximum SO_2 removal efficiency reached up to 84.5%. © 2014 American Institute of Chemical Engineers *AIChE J*, 60: 2298–2306, 2014

Keywords: sulfur dioxide removal efficiency, polyetherimide, poly(vinyl chloride)-graft-poly(oxyethylene methacrylate), second flue gas desulfurization, composite hollow fiber membrane

Introduction

The emission of carbon dioxide (CO_2) from the combustion of fossil fuels has been identified as a major contributor to global warming and climate change. CO_2 capture and storage (CCS) has been suggested as a method to reduce CO_2 emissions from power plants. Although various processes have been investigated for the capture of CO_2 from flue gas, selective absorption using an amine-based solvent is the most promising technology because it is well suited for retrofitting existing plants.[1] The minor components of flue gas from coal power plants contain SO_X, NO_X, Hg and so forth. In particular, emission gas from coal-power plant which treated by wet flue gas desulfurization (FGD) system.[2] In the flue gas stream, the sulfur dioxide (SO_2) concentration is in the range of 6–300 ppm after wet desulfurization.[3] The SO_2 react with amine-based solvents in the CCS process to form heat-stable salts that reduce the CO_2 absorption capacity.[4] Thus, the very low concentration of SO_2 concentration are desirable to avoid excessive loss of costly solvent.[5] Therefore, the emission system requires an enlargement of the process scale or an improvement in the filler and the column structure to reach the emission standard. However, this requires additional supplies and equipment for the circulation of liquid sorbents. Hence, many researchers have been studying the possibilities of new, upgraded separation process through the technology combination. In this study, suggested the membrane separation process to achieve additional SO_2 removal efficiency from the flue gas after the first FGD. Compared to conventional separation process, the membrane process has economical advantages because of its process compaction and low-energy demand. Furthermore, this method can flexibly respond to operating conditions and is easy to control.[6–8] Many researchers have accordingly studied SO_2 permeation properties using polymeric membranes. In 1975, Felder et al.[9] investigated the permeation of SO_2 through various polymers. They summarized the effects of gas pressure,

Correspondence concerning this article should be addressed to H. Lee at hklee@kier.re.kr.

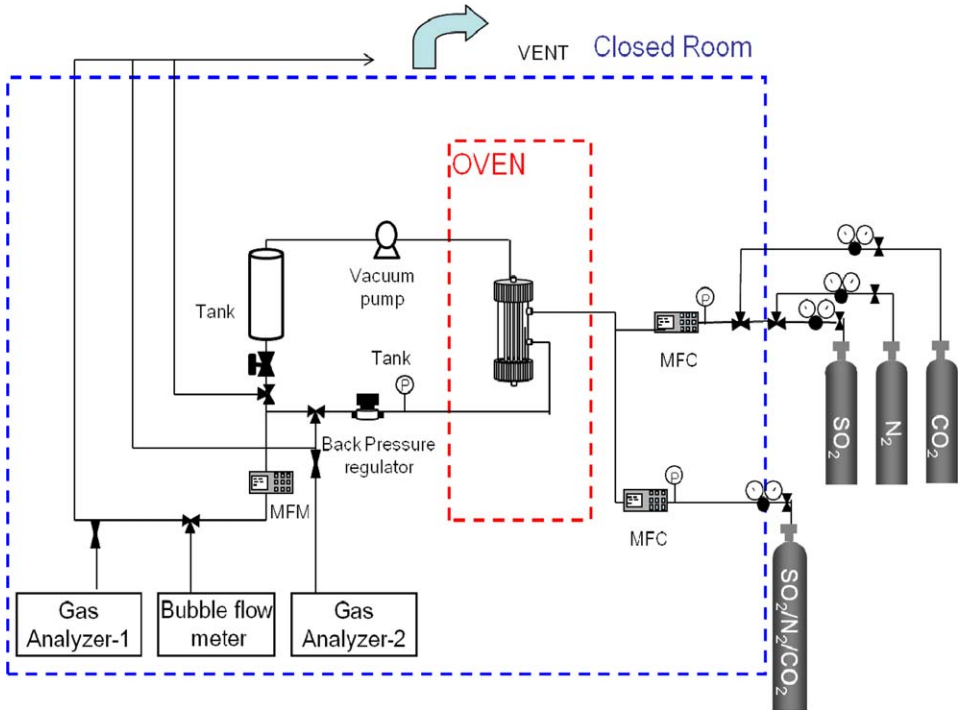

Figure 1. Schematic diagram of gas permeation experiment apparatus.

[Color figure can be viewed in the online issue, which is available at wileyonlinelibrary.com.]

humidity, and membrane plasticization on SO_2 permeabilities. In addition, Yampol'skii et al.[10] studied the permeability of SO_2 through a continuous and asymmetrical polyvinyl trimethylsilane membrane at various operating conditions (pressure and temperature). Scholes et al.[11] investigated SO_2 permeability and SO_2/CO_2 selectivity for a number of polymeric membranes. Recently, Ren et al.[12] reported research work on sour gas (CO_2, H_2S, and SO_2) separation from a nonpolar gas using a flat sheet composite membrane that was prepared with polyetherimide (PEI) and poly(ether-*b*-amide) (PEBAX). PEBAX shows high sour gas permeability and a high selectivity for polar gas/nonpolar gas separation because it contains a hydrophilic polyethyleneoxide segment in the polymer chain.

This study aims to develop the composite membrane using for separation of low concentration of SO_2 from the mixed gas. Poly(vinyl chloride)-graft-poly(oxyethylene methacrylate) (PVC-*g*-POEM) was synthesized via the atom transfer radical polymerization (ATRP) method using direct initiation of the secondary chlorines of PVC. The flat sheet PVC-*g*-POEM membrane performed high permeability and selectivity to polar/nonpolar gas mixture separation due to the ether group in POEM.[13]

For large scale applications, the hollow fiber configuration is more beneficial than the flat sheet membrane because of its higher packing density, good self mechanical support, and easy handling during the module fabrication and process operation.[14,15] The composite membrane composed of a thick, porous, nonselective support layer, and a thin selective layer has some advantages over the asymmetric materials and each layer can be manipulated independently to obtain optimal separation performance.[16] Ideally, the selective layer which is usually an expensive high performance polymer, controls the flux and selectivity of the composite membrane. The porous support substrate is to provide the mechanical strength for the selective layer in high operational pressure, and it does not contribute to the transport of the gas. The most attractive aspect of composite structures is their potential for minimizing cost because an only small quantity of the high performance polymer is utilized for its formation.[17]

In this study, a hollow fiber composite membrane was prepared by PVC-*g*-POEM coating on a PEI substrate. PEI was chosen for the preparation of a hollow fiber membrane (HFM) substrate because it is composed of aromatic imide units and provides stiffness, chemical resistance, and flexible ether linkages which in turn offer good ability to easily fabricate the HFM.[18,19] The manufactured PVC-*g*-POEM/PEI hollow fiber composite membrane was characterized using scanning electron microscopy (SEM), Fourier transform infrared spectroscopy (FTIR), and atomic force microscopy (AFM). Then, the gas permeation properties were investigated by single gas permeation and mixed gas separation experiment.

Experimental

Fabrication of PEI HFM

HFM were produced by a dry/wet phase inversion method.[20] The dope solution composed with 25.0 wt % PEI (Ultem 1000, General Electric), 62.5 wt % N-methylpyrrolidone (NMP, Merck, Germany), and 12.5 wt % ethanol (SAMCHUN PURE CHEMICAL, Korea). The detailed description of spinning procedures has been elaborated elsewhere.[21] In this work, the dope solution and internal coagulant (DI water) were passed through a double pipe spinneret having 0.12/0.6 mm inner/outer diameter and the air gap maintained at 2.0 cm.

Preparation of PVC-g-POEM/ PEI hollow fiber composite membrane

Poly (vinyl chloride) (PVC) is one of the most widely used vinyl polymers in the world because of its low cost, easy process ability, and recyclability. However, PVC

Table 1. Physical Properties of SO_2, CO_2, and N_2

	Molecular Weight (g mol^{-1})	Kinetic Diameter (Å)	Critical Temperature (K)	Critical Volume (cm^3 mol^{-1})	Critical Pressure (kPa)
SO_2	64.1	3.60	430.8	122.0	7780
CO_2	44.0	3.30	304.0	93.9	7290
N_2	28.0	3.64	126.2	89.8	3360

membranes exhibit low permeability for gas separation due to their high chain compactness and the low segmental motion of the polymeric chain.[22] PVC synthesized with POEM presents high affinity for polar gases such as SO_2. The PVC-*g*-POEM synthesis method was explained in elsewhere.[23] A nascent PEI HFM was coated with PVC-*g*-POEM (POEM 86 wt %, $M_w = 155{,}819$ g mol^{-1}) to enhance the permeability and selectivity.[24] The synthesized graft copolymer (2.0 wt %) was dissolved in acetone at 313 K for 8 h. After cooling the solution at room temperature, it was coated on the outer surface of PEI HFM using a continuous coating system. The nascent PEI HFM was passed through the PVC-*g*-POEM coating solution and dried at 343 K.

Characterization of the membranes

The fiber was examined by scanning electron microscope (SEM, S-4700, Hitachi). Hollow fiber samples were fractured in liquid nitrogen and coated with gold using a sputter coater before the SEM observation. Measurement of the FTIR to understand the surface chemistry of the composite membrane was performed using an ALPHA-P Spectrometer with a diamond ATR cell (Bruker) at 600–4000 cm^{-1}. AFM was used for the verification of morphology changes caused by PVC-*g*-POEM coating. The values of roughness were obtained using a Nanoman AFM system (Veeco) in tapping mode.

Gas permeation measurement

The experimental setup for the single gas permeation and the mixed gas separations are shown in Figure 1. Two hundred pieces of composite hollow fibers were potted to form a module. The fibers were 26-cm long, and the effective area of the membrane was 718.8 cm^2. To determine the single gas permeance, the module was permeated with pure gas SO_2 (99.98%, SAFETY GAS, Korea), CO_2 (99.5%, SAFETY GAS, Korea), and N_2 (99.999%, SAFETY GAS, Korea) with a range in pressure difference of 50–500 kPa and temperature of 303–343 K. Because of the condensability of SO_2, its permeance was measured until 250 kPa. The physical properties of the single gases are listed in Table 1.

Gas permeation rate was measured using a bubble flow meter. Gas permeance can be described by the universal equation

$$P = \frac{Q_p}{A \cdot \Delta p} \tag{1}$$

where Q_p is the gas permeation rate through the membrane, Δp is the gas pressure difference across the membrane, and A is the effective membrane area. Permeance (P) was expressed in gas permeation unit (GPU) was defined as Eq. 2

$$1\text{GPU} = 1\times10^{-6}\frac{\text{cm}^3(\text{STP})}{\text{cm}^2\times\ \text{cm Hg}\ \times\ \text{s}} \tag{2}$$

The ideal selectivity was determined by taking the ratio of the pure gas permeances

$$\alpha_{i/j} = P_i/P_j \tag{3}$$

For separation of a gas mixture, a $SO_2/CO_2/N_2$ mixture of 200 ppm of SO_2, 11.98% of CO_2, and N_2 balanced gas was used. The effects of various operating conditions such as pressure, temperature, and stage cut were investigated. All measurements were recorded when the system reached a steady state at specific conditions. The pressure and retentate flow rate were managed by a back pressure regulator. The buffer tank was installed behind the pump in order to minimize pulsation. A gas analyzer (A02020, The ABB, Germany) was used to detect the concentration of SO_2 and CO_2 at the permeate and retentate stream. The mixed gas was fed to the shell side of the HFM and a vacuum pump were connected to the permeate stream that provided the required vacuum (20 kPa) to minimize the pressure drop developed during the permeation experiments. The flow rate of the permeate stream will be less than that of the feed stream so that the ideal energy consumption of a vacuum pump on the permeate side will be less than that of a feed compressor for the same pressure ratio.[25] A permeate pressure of <20 kPa may not be feasible with state-of-the-art industrial scale vacuum pumps.[26] As shown in Eq. 4, stage cut can be expressed as the ratio of permeate flow rate and feed flow rate. Feed flow rate can be expressed as the sum of the retentate flow (Q_R) and permeate flow rate (Q_P)

$$\theta = \frac{Q_P}{Q_P + Q_R} \tag{4}$$

The separation factor (π) can be calculated as Eq. 5

$$\pi = \frac{(C_i/C_j)_{\text{Permeate}}}{(C_i/C_j)_{\text{Feed}}} \tag{5}$$

where C_i and C_j represent the concentrations of gas i and j, respectively. The separation factor is the ratio of the compositions of components i and j in the permeate stream relative to the composition ratio of these component in the feed stream.

The SO_2 removal efficiency (η) can be calculated by Eq. 6

$$\eta(\%) = \left(1 - \frac{C_{i,R}}{C_{i,F}}\right)\times100 \tag{6}$$

where $C_{i,F}$ and $C_{i,R}$ are the concentrations (ppm) of the SO_2 in the feed and retentate streams, respectively.

Results and Discussion

Characterization of composite membranes

In this study, the dry/wet phase inversion method was used to fabricate HFM. The structure and the geometrical characteristics of the produced HFM were studied by SEM as shown in Figure 2. The produced fiber typically has an asymmetric structure (Figure 2a); a dense top layer supported by porous, sponge, and finger-like substructure. The PVC-*g*-POEM selective layer provides high selectivity with a low resistance to permeance of polar gases while the porous substructure provides mechanical strength to the fiber

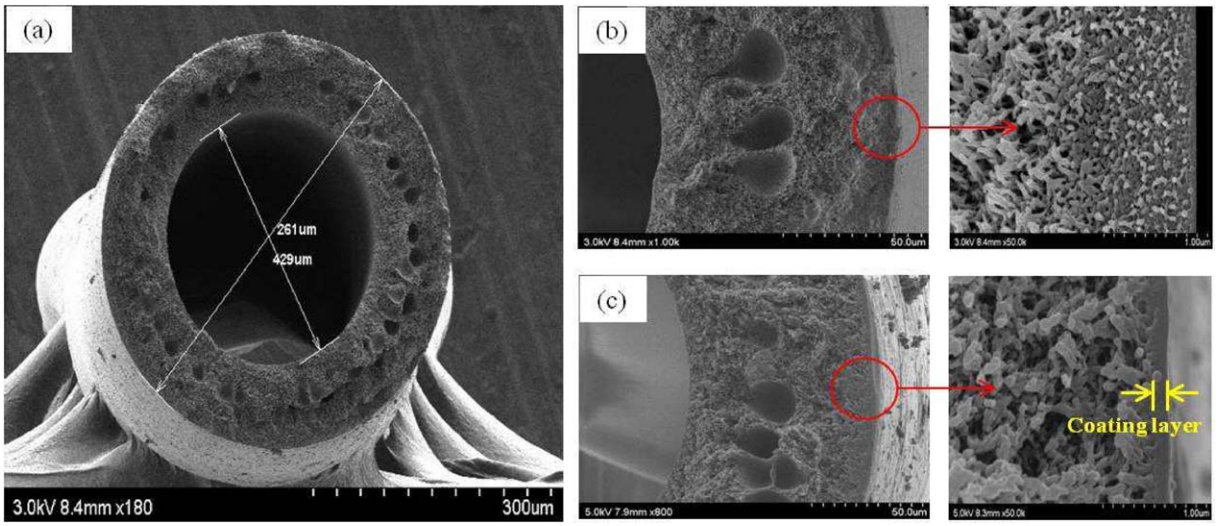

Figure 2. SEM images of the PEI HFM.

(a) Overall cross-section, (b) partial cross-section of PEI substrate, and (c) PVC-*g*-POEM/PEI composite membrane. [Color figure can be viewed in the online issue, which is available at wileyonlinelibrary.com.]

for high-pressure application.[27] The inner and outer diameters of the HFM are 261 and 429 μm, respectively. The distinguishable boundary between the coating layer and the substrate is noted. The morphological changes before and after the coatings of PVC-*g*-POEM are shown in Figures 2b, c, respectively. A selective coating layer (∼0.1 μm) was clearly seen on the outer surface of PEI substrate membrane as illustrated in Figure 2c.

The AFM analysis was carried out to the observation of coating layer. Figure 3 presents the typical AFM images of the surface topography before (Figure 3a) and after (Figure 3b) dynamically coating with PVC-*g*-POEM. The nodules are characterized by the high peaks seen as bright regions in the AFM images.[28] After coating on the surface of support membrane, the belt-like structure can be observed as shown in Figure 3. The surface roughness parameters of PEI support and PVC-*g*-POEM coated membrane obtained from AFM images are summarized in Table 2. The roughness parameters expressed in terms of the mean roughness (Ra), the mean-square roughness (Rq), and the mean difference between highest peak and lowest valley (Rz). The values of roughness parameter (Ra, Rq, and Rz) were increased with PVC-*g*-POEM coating due to the surface enrichment of PVC-*g*-POEM. The surface of composite membrane formed has a "ridge-and-valley" morphology that gives quantitatively rougher surface morphology.[29]

The FTIR spectra of PEI substrate and PVC-*g*-POEM composite membrane are displayed in Figure 4. PEI substrate has two strong peak for the imide carbonyl group at 1778 and 1721 cm^{-1}. Also, it exhibits characteristic at 1356 and 744 cm^{-1} (C—N stretching and bending) and at 1236 cm^{-1} (aromatic ether C—O—C).[30] The composite membrane exhibited the strong stretching band in 2875, 1720, and 1103 cm^{-1} due to graft copolymerization of coating solution. These bands result from the stretching vibration modes of methyl (CH_2), carbonyl (C═O), and ether bond (C—O—C) of POEM, respectively.[19]

Single gas permeance of composite membrane

Figure 5 presents the permeance of single gas according to pressure and temperature. The permeance of SO_2

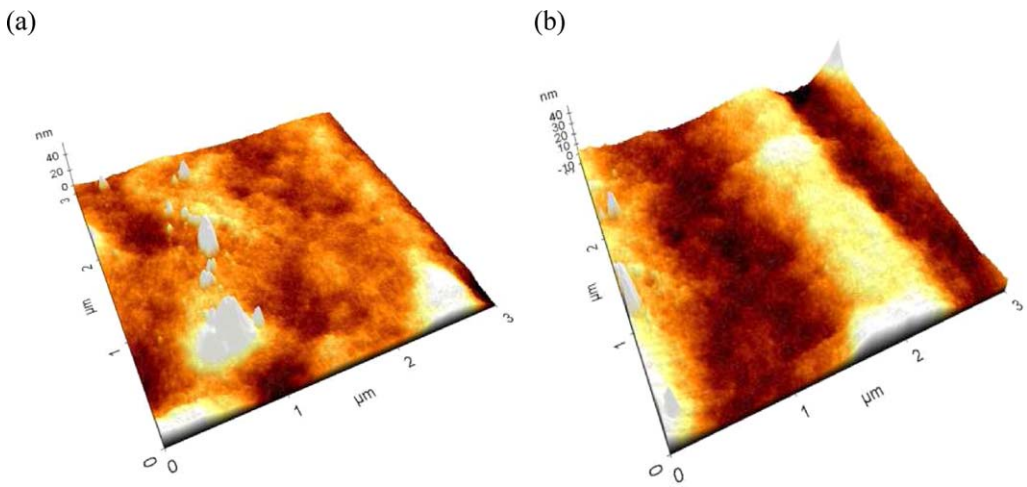

Figure 3. AFM images of the HFMs.

(a) PEI substrate and (b) PVC-*g*-POEM/PEI composite membrane. [Color figure can be viewed in the online issue, which is available at wileyonlinelibrary.com.]

Table 2. Surface Roughness Parameters of PEI Support and PVC-*g*-POEM/PEI Composite Membrane

	Roughness		
Membrane	Ra (nm)	Rq (nm)	Rz (nm)
PEI support	2.68	4.82	35.41
PVC-*g*-POEM/PEI	4.16	5.11	56.23

enhanced up to 2705 GPU at 250 kPa. In contrary, it decreased steeply with an increasing temperature from 303 to 343 K. Usually, gas solubility increases with the increasing condensability characterized by critical temperature while the gas diffusivity decreases with the increase of critical volume.[31] Although SO_2 has a larger kinetic diameter than CO_2, it has higher critical temperature that means it can be easy to penetrate through the membrane. Permeance of SO_2 increased steeply at 303 K due to the plasticization. According to the "plasticization phenomenon," a condensable gas usually causes swelling of the polymer matrix and reduces the interaction between the adjacent segments of polymer chains, consequently increasing the segmental mobility and free volume. As a result, an increase in permeance is commonly observed.[32] Typically, as gas critical temperature increases, activation energies of permeation decrease monotonically.[33]

In the case of CO_2 and N_2, as shown in Figure 5b, the permeance of CO_2 increased with increasing pressure while that of N_2 was essentially independent of pressure. However, the permeances of both CO_2 and N_2 were enhanced with increasing temperature. As a result, the selectivity of SO_2/CO_2 increased with pressure, whereas it showed the opposite trend in the case of temperature, as shown in Figure 6.

Basically, the transport of a gas through the polymeric membrane can be described in terms of a solution-diffusion mechanism.[34] Solubility is a thermodynamic parameter and gives a measure of the amount of penetrant sorbed by the membrane under equilibrium conditions. As the permeability depends on both solubility and diffusivity, parameters must be involved to understand the temperature effect.[35] Temperature dependency of permeance can be explained through the Arrhenius relation shown in Eq. 7

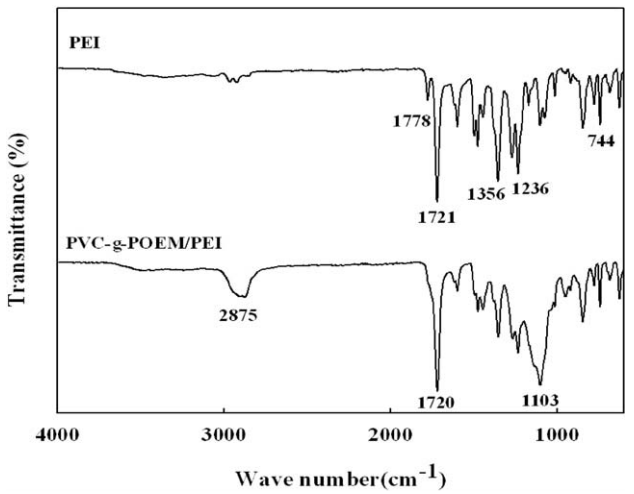

Figure 4. FTIR spectra of PEI and PVC-*g*-POEM/PEI composite membrane.

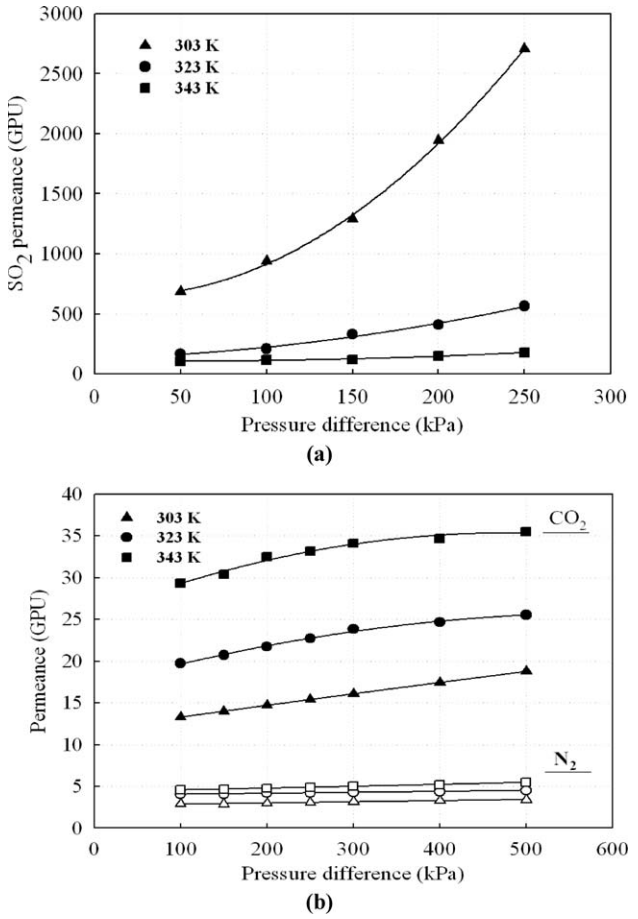

Figure 5. Single gas permeance according to pressure and temperature difference.

$$P = P_0 \exp\left(-\frac{E_P}{RT}\right) \tag{7}$$

P_0 denotes a pre-exponential factor and E_P is the activation energy (kJ mol^{-1}) for permeation. The activation energy for permeation comprises of the activation energy for diffusion and the heat of sorption

$$\Delta E_P = \Delta E_D + \Delta H_S \tag{8}$$

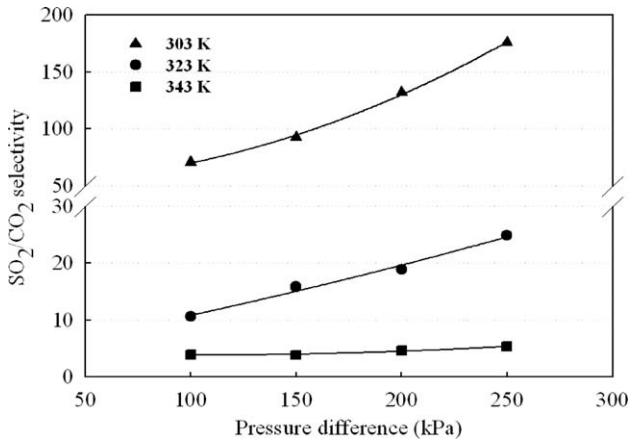

Figure 6. SO2/CO2 ideal selectivity according to pressure and temperature difference.

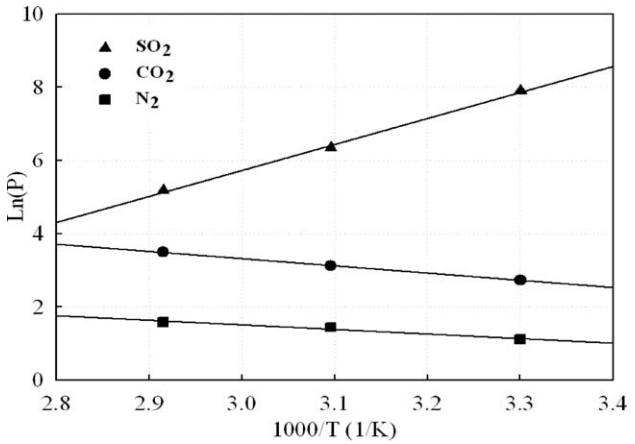

Figure 7. Arrhenius plot of single gas permeance.

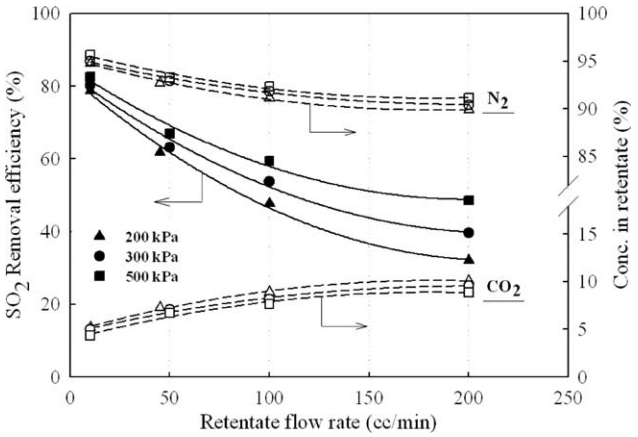

Figure 8. Experiment results of SO2 removal efficiency and CO2, N2 concentration in retentate stream depending on the pressure difference.

Diffusivity always increases with increasing temperature, that is, the energy of activation for diffusion is positive ($\Delta E_D > 0$). Conversely, solubility increases with decreasing temperature, that is, the heat of solution is negative ($\Delta H_S < 0$).[36]

Figure 7 presents an Arrhenius plot of single gas permeance at 303 K and 250 kPa operating pressure. The slope of the linear fitting curve was used to calculate their activation energy for permeation. The activation energies of the gases were -59.1 kJ mol^{-1} of SO_2, 16.1 kJ mol^{-1} of CO_2, and 10.2 kJ mol^{-1} of N_2, respectively. The negative activation energy indicates that the solution is dominant in the permeation of SO_2. In other words, an increase of temperature leads to a decrease of permeance, as shown in Figure 5a. The free volume of the polymeric membrane was affected by the inherent condensability of the penetrant.

For condensable gases, the heat of sorption term is negative and the solubility decreases with increasing temperature. Therefore, an increase of temperature induces a decrease of SO_2 solubility due to the large heat of sorption, which dominates the permeation process of SO_2. However, the values of permeance for CO_2 and N_2 increase exponentially with increasing temperature. This indicates that the temperature dependence of permeance for CO_2 and N_2 in this membrane is dominated by diffusion.[37] However, the experimental data show that the activation energy of CO_2 decreased despite its high critical temperature because the increase in the CO_2 diffusivity compensated the decrease of the solubility parameter at the given experimental conditions.[38] In contrast to the activation energy of N_2, that of CO_2 decreased with pressure (Table 3). The condensable gases such as SO_2 and CO_2, diffusion processes are always enhanced as the increase of temperature. However, the increase of temperature will lead to an increase of the saturated vapor pressure of condensable gases, resulting in their lower activity.[12] An increase of operating pressure induces stronger plasticization of the polymer chain, followed by a fractional free volume increase with a decrease of diffusion activation energy. This indicates that the permeation of CO_2 under investigation shows that diffusivity was controlled at low pressure and solubility was controlled at higher pressure.[39]

Table 3. Activation Energy of Composite Hollow Fiber Membrane (Unit: kJ/mol)

Penetrant	100 kPa	200 kPa	250 kPa	400 kPa	500 kPa
SO_2	−45.9	−55.4	−59.1	–	–
CO_2	18.2	17.1	16.1	14.8	13.8
N_2	10.0	10.1	10.2	10.3	10.3

Mixed gas separation of composite membrane

Figures 8 and 9 present the results of a mixed gas separation experiment as a function of the retentate flow rate and pressure difference at a fixed temperature of 303 K. According to Eq. 4, an increase of the retentate flow rate suggests a reduction of the stage cut. At fixed pressures, the stage cut decreased as the retentate flow rate increased due to the increasing feed flow rate. Otherwise, when the stage cut increases, the concentration of the gas with low permeance increases because the driving force of penetrants against the membrane increases.[40] Therefore, the concentrations of SO_2 and CO_2 in the retentate stream were enhanced with an increased retentate flow rate and vice versa, whereas the concentration of N_2 decreased as shown in Figure 8.

The permeate flow rate was enhanced due to an increase of permeate driving force. Also, the flexibility of the polymer chains was increased by the plasticization effect, which occurs due to condensable gas in the mixture, and thus the

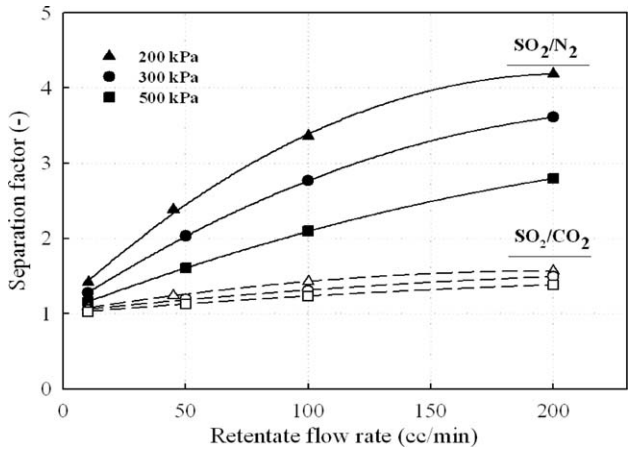

Figure 9. Experiment results of separation factor depending on the pressure difference.

permeation flux increased.[41] The effect of operating pressure on the gas permeance and selectivity can be verified from single gas experiment results. Similarly, SO_2 removal efficiency was improved and the concentration of CO_2 in the retentate stream was decreased due to the increase of operating pressure while the retentate flow rate was maintained.

Figure 9 illustrates the results of the separation factor, estimated from Eq. 5. The separation factor is defined as the change of gas concentration of species that permeate faster than others in the mixed gas between the feed and permeate stream. It is important to well distinguish between ideal selectivity and the separation factor. The ideal selectivity calculated from the pure gas permeances measured in ideal conditions and it represents a property of the material. The separation factor indicates the actual performance of the membrane module and it depends on the operating conditions such as pressure, temperature, stage cut, and mixture composition.[42] The separation factors are significantly lower than ideal selectivities of the pure gases due to the competition for sorption sites by the penetrants. The availability of sorption sites for each component is reduced due to the presence of the other components; thus, the permeation rate for each component is also decreased in comparison with the corresponding pure gas permeation rate.[43,44] The separation factors increased with increasing retentate flow rate, because N_2 has a lower permeation rate than the other components. Conversely, the separation factors decreased with the pressure increase. As mentioned before, permeate driving force in the membrane process is enhanced by increasing the pressure. As a result, it generates coercive permeation, and all of the species in the mixture gas are thereby easily permeated. In addition, the N_2 portion of 88 vol % in the feeding mixture gas interrupts the permeation of other gases. Therefore, the concentration of N_2 in permeate stream increased relative to that of SO_2. This is also shown in the calculation of SO_2/CO_2 separation factor.

Figures 10 and 11 present the mixed gas separation results depending on the retentate flow rate and temperature difference at 200 kPa of operating pressure. Figure 10 shows that the SO_2 removal efficiency reduced with decreasing temperature. In the results of single gas permeation experiments, the permeance of SO_2 was decreased with increased temperature whereas that of N_2 was increased. However, the mixed gas separation result shows that the concentration of SO_2 was enhanced in the permeate stream by increasing the operating temperature. This result can be explained by taking competitive sorption and concentration polarization into account. Concentration polarization means that a concentration gradient is building up due to depletion of the more permeable component and accumulation of the less permeable species in the boundary layer adjacent to the membrane.[41] The permeation properties of the gas mixture were dominated by diffusivity because the gas was mainly composed of N_2. Increasing the temperature significantly affected the diffusivity of each gas in the mixture as shown in Figure 7. Permeation flux was increased by temperature due to an enhancement of N_2 diffusivity.[45] Elevated temperatures increase the N_2 flux which reduces the effect of the concentration polarization. With the effect of concentration polarization reduced, more SO_2 and CO_2 can permeate through the membrane. As a result, the SO_2 removal efficiency improved as the temperature increased.

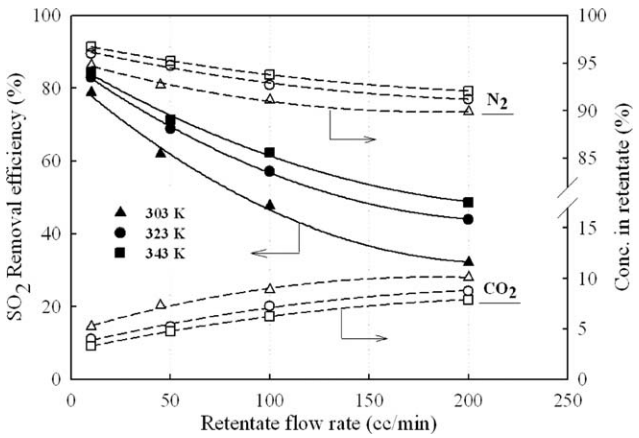

Figure 10. Experiment results of SO2 removal efficiency and CO2, N2 concentration in retentate stream depending on the temperature difference.

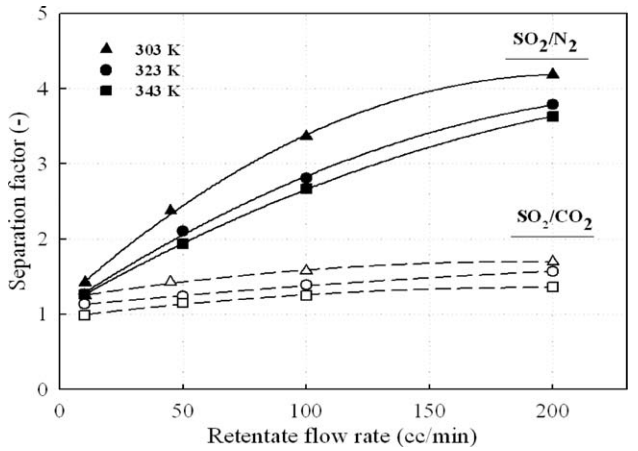

Figure 11. Experiment results of separation factor depending on the pressure difference.

Figure 11 shows the separation factor of gas pairs using the mixed gas. The cause of these tendencies can be confirmed by the single gas activation energy results. The activation energy of SO_2 had a negative value, whereas the other gases (CO_2 and N_2) showed positive values at 200 kPa of operating pressure as listed in Table 3. Therefore, the concentration of SO_2 in the permeate stream was decreased and also, the separation factor of SO_2/N_2 and SO_2/CO_2 were decreased according to increasing temperature. The permeation of SO_2 is significantly affected by presence of other penetrant because it contains relatively low concentration (200 ppm) in the mixed gas.[46] Hence, the SO_2 concentration in the permeate stream significantly affected by the effect of penetrant competition, gas phase nonideality, plasticization phenomena, and gas polarization.

Conclusions

In this study, a PEI HFM was produced by the dry/wet phase inversion method. The nascent membrane was coated with PVC-*g*-POEM, which was synthesized by ATRP. The composite membrane was characterized by SEM, FTIR, and AFM. Pure gas of SO_2, CO_2, and N_2 were tested to calculate

single gas permeance. The results indicate that the permeance of SO_2 increased under the operating pressure while that of N_2 was essentially independent of any pressure change. However, selectivity decreased with increasing temperature due to the different permeation mechanisms. The permeance of SO_2 was affected by solubility, whereas CO_2 and N_2 were dominated by diffusivity under the operating conditions. These results can be predicted from the Arrhenius equation.

SO_2 (200 ppm), 12% of CO_2, and a N_2 balanced mixed gas was used for the separation test, here removal efficiency was evaluated a function of the operating pressure, temperature, and retentate flow rate, respectively. SO_2 removal efficiency improved according to increasing pressure due to the enhancement of the permeate flux. Moreover, increasing temperature had a significant effect on the diffusivity of single gases in the mixture. The effect of compatible sorption is mitigated by suppression of concentration polarization. Consequently, increasing pressure and temperature advantageously affected SO_2 separation from the $SO_2/CO_2/N_2$ mixed gas, and the SO_2 removal efficiency consequently reached 84.5%.

Literature Cited

1. Mores P, Rodríguez N, Scenna N, Mussati S. CO_2 capture in power plants: minimization of the investment and operating cost of the post-combustion process using MEA aqueous solution. *Int J Greenhouse Gas Control*. 2012;10:148–163.
2. Uyanga IJ, Idem RO. Studies of SO_2-and O_2-induced degradation of aqueous MEA during CO_2 capture from power plant flue gas stream. *Ind Eng Chem Res*. 2007;46:2558–2566.
3. Yang J, Yu X, Yan J, Tu ST, Dahquist E. Effect of SO_2 on CO_2 capture using a hollow fiber membrane contactor. *Appl Energy*. 2013;112:755–764.
4. Stanger R, Wall T. Sulphur impacts during pulverised coal combustion in oxy-fuel technology for carbon capture and storage. *Prog Energy Combust Sci*. 2011;37:69–88.
5. Rao AB, Rubin ES. A technical, economic, and environmental assessment of amine-based CO_2 capture technology for power plant greenhouse gas control. *Environ Sci Technol*. 2002;36:4467–4475.
6. Car A, Stropnik C, Yave W, Peinemann KV. PEG modified poly (amide-b-ethylene oxide) membranes for CO_2 separation. *J Membr Sci*. 2008;307:88–95.
7. Ahn JS, Lee SM. A study on the separation characteristics of CH_4-CO_2 mixed gas by polyimide hollow fiber membrane. *Korean Chem Eng Res*. 1996;34:675–682.
8. Park HH, Deshwal BR, Jo HD, Choi WK, Kim IW, Lee HK. Absorption of nitrogen dioxide by PVDF hollow fiber membranes in the G-L contactor. *Desalination*. 2009;243:52–64.
9. Felder RM, Spence RD, Ferrell JK. Permeation of sulfur dioxide through polymers. *J Chem Eng Data*. 1975;20:235–242.
10. Yampol'skii YP, Volkov VV, Kalyuzhnyi NE, Durgar'yan SG. Permeability, diffusion and sorption of SO_2 in polyvinyltrimethyl silane membranes. *Polym Sci USSR*. 1984;26:1832–1840.
11. Scholes CA, Kentish SE, Stevens GW. Effect of minor components in carbon dioxide capture using polymeric gas separation membranes. *Sep Purif Rev*. 2009;38:1–44.
12. Ren X, Ren J, Deng M. Poly(amide-6-b-ethylene oxide) membranes for sour gas separation. *Sep Purif Technol*. 2012;89:1–8.
13. Ahn SH, Seo JA, Kim JH, Ko YD, Hong SU. Synthesis and gas permeation properties of amphiphilic graft copolymer membranes. *J Membr Sci*. 2009;345:128–133.
14. Sukitpaneenit P, Chung TS. Fabrication and use of hollow fiber thin film composite membranes for ethanol dehydration. *J Membr Sci*. 2014;450:124–137.
15. Zhang L, He G, Zhao W, Nie F, Li X, Tan M. Studies on the coating later in a PTFPMS/PEI composite membrane for gaseous separation. *J Membr Sci*. 2011;371:141–147.
16. Zhao J, Wang Z, Wang J, Wang S. Influence of heat-treatment on CO_2 separation performance of novel fixed carrier composite membranes prepared by interfacial polymerization. *J Membr Sci*. 2006;283:346–356.
17. Hamad F, Khulbe KC, Matsuura T. Comparison of gas separation performance and morphology of homogeneous and composite PPO membranes. *J Membr Sci*. 2005;256:29–37.
18. Zhang L, He G, Zhao W, Tan M, Li X. Effect of formamide additive on the structure and gas permeation performance of polyetherimide membrane. *Sep Purif Technol*. 2010;73:188–193.
19. Kneifel K, Peinemann KV. Preparation of hollow fiber membranes from polyetherimide for gas separation. *J Membr Sci*. 1992;65:295–307.
20. Kim DH, Baek IH, Hong SU, Lee HK. Study on immobilized liquid membrane using ionic liquid and PVDF hollow fiber as a support for CO_2/N_2 separation. *J Membr Sci*. 2011;372:346–354.
21. Park HH, Deshwal BR, Kim IW, Lee HK. Absorption of SO_2 from flue gas using PVDF hollow fiber membranes in a gas-liquid contactor. *J Membr Sci*. 2008;319:29–37.
22. Bierbrauer K, López-González M, Riande E, Mijangos C. Gas transport in fluorothiophenyl modified PVC membranes. *J Membr Sci*. 2010;362:164–171.
23. Koh JH, Lee KJ, Seo JA, Kim JH. Amphiphilic polymer electrolytes consisting of PVC-g-POEM comb-like copolymer and $LiCF_3SO_3$. *J Polym Sci Part B: Polym Phys*. 2009;47:1443–1451.
24. Roh DK, Park JT, Ahn SH, Ahn HJ, Ryu DY, Kim JH. Amphiphilic poly(vinyl chloride)-g-poly(oxyethylene methacrylate) graft polymer electrolytes: interactions, nanostructures and applications to dye-sensitized solar cells. *Electrochim Acta*. 2010;55:4976–4981.
25. Bounaceur R, Lape N, Roizard D, Vallieres C, Favre E. Membrane process for post-combustion carbon dioxide capture: a parametric study. *Energy*. 2006;31:2556–2570.
26. Ramasubramamian K, Verweij H, Ho WSW. Membrane processes for carbon capture from coal-fired power plant flue gas: a modeling and cost study. *J Membr Sci*. 2012;421–422:299–310.
27. Kosuri MR, Koros WJ. Defect-free asymmetric hollow fiber membranes from Torlon®, a polyamide-imide polymer, for high-pressure CO_2 separation. *J Membr Sci*. 2008;320:65–72.
28. Khayet M, Feng CY, Khulbe KC, Matsuura T. Preparation and characterization of polyvinylidene fluoride hollow fiber membranes for ultrafiltration. *Polymer*. 2002;43:3879–3890.
29. Corneal LM, Masten SJ, Davies SHR, Tarabara VV, Byun S, Baumann MJ. AFM, SEM and EDS characterization of manganese oxide coated ceramic water filtration membranes. *J Membr Sci*. 2010;360:292–302.
30. Chen BK, Su CT, Tseng MC, Tsay SY. Preparation of polyetherimide nanocomposites with improved thermal, mechanical and dielectric properties. *Polym Bull*. 2006;57:671–681.
31. Liu L, Chakma A, Feng X. Preparation of hollow fiber poly(ether block amide)/polysulfone composite membranes for separation of carbon dioxide from nitrogen. *Chem Eng J*. 2004;105:43–51.
32. Dong G, Li H, Chen V. Plasticization mechanisms and effects of thermal annealing of Matrimid hollow fiber membranes for CO_2 removal. *J Membr Sci*. 2011;369:206–220.
33. Merkel TC, Gupta RP, Turk BS, Freeman BD. Mixed-gas permeation of syngas components in poly(dimethylsiloxane) and poly(1-trimethylsilyl-1-propyne) at elevated temperatures. *J Membr Sci*. 2001;191:85–94.
34. Scholes CA, Kentish SE, Stevens GW. Carbon dioxide separation through polymeric membrane system for flue gas applications. *Recent Pat Chem Eng*. 2008;1:52–66.
35. Powell CE, Qiao GG. Polymeric CO_2/N_2 gas separation membranes for capture of carbon dioxide from power plant flue gases. *J Membr Sci*. 2006;279:1–49.
36. Mulder M. *Basic Principles of Membrane Technology*, 2nd ed. Netherland: Kluwer academic publishers, 1996.
37. Mohammadi T, Moghadam MT, Saeidi M, Mahdyarfar M. Acid gas permeation behavior through poly(ester urethane urea) membrane. *Ind Eng Chem Res*. 2008;47:7361–7367.
38. Francisco GJ. Separation of carbon dioxide from nitrogen using poly(vinyl alcohol)-amine blend membranes. PhD Thesis. Waterloo: University of Waterloo, 2006.
39. Zavaleta R, McCandless FP. Selective permeation through modified polyvinylidene fluoride membranes. *J Membr Sci*. 1976;1:333–353.
40. Ho WSW, Sirkar KK. *Membrane Handbook*. New York: Van Nostrand Reinhold, 1992.
41. Kanehashi S, Nakagawa T, Nagai K, Duthie X, Kentish S, Stevens G. Effect of carbon dioxide-induced plasticization on the gas

transport properties of glassy polyimide membranes. *J Membr Sci*. 2007;298:147–155.
42. Peer M, Kmali SM, Mahdeyarfar M, Mohammadi T. Separation of hydrogen from carbon monoxide using a hollow fiber polyimide membrane: experimental and simulation. *Chem Eng Technol*. 2007;30:1418–1425.
43. Choi SH, Brunetti A, Drioli E, Barbieri G. H_2 Separation from H_2/N_2 and H_2/CO mixtures with co-polyimide hollow fiber module. *Sep Sci Technol*. 2011;46:1–13.
44. David OC, Gorri D, Nijmeijer K, Ortiz I, Urtiaga A. Hydrogen separation from multicomponent gas mixtures containing CO, N_2 and CO_2 using Matrimid® asymmetric hollow fiber membranes. *J Membr Sci*. 2012;419–420:49–56.
45. Sadrzadeh M, Amirilargani M, Shahidi K, Mohammadi T. Pure and mixed gas permeation through a composite polydimethylsiloxane membrane. *Polym Adv Technol*. 2011;22:586–597.
46. Chen XY, Rodrigue D, Kaliaguine S. Diamino-organosilicone APTMDS: a new cross-linking agent for polyimides membranes. *Sep Purif Technol*. 2012;8:221–233.

Manuscript received Oct. 18, 2013, and revision received Jan. 29, 2014.